

Enhanced detectability of community structure in multilayer networks through layer aggregation

Dane Taylor,^{1,*} Saray Shai,¹ Natalie Stanley,^{1,2} and Peter J. Mucha¹

¹*Carolina Center for Interdisciplinary Applied Mathematics,*

Department of Mathematics, University of North Carolina, Chapel Hill, NC 27599, USA

²*Curriculum in Bioinformatics and Computational Biology, Chapel Hill, NC 27599, USA*

Community detection is a central pursuit for understanding the structure and function of biological, social and technological networks, and it is important to understand the fundamental limitations on detectability. Many systems are naturally represented by a multilayer network in which edges exist in multiple layers that encode different—but potentially related—types of interactions. Using random matrix theory for stochastic block models, we analyze detectability limitations for multilayer networks and find that by aggregating together similar layers, it is possible to identify structure that is undetectable in a single layer. We explore this phenomenon for several aggregation methods including summation of the layers’ adjacency matrices, for which detectability limit vanishes with increasing number of layers, L , decaying as $\mathcal{O}(L^{-1/2})$. Interestingly, we find a similar scaling behavior when the summation is thresholded at an optimal value, supporting the common—but not well understood—practice of thresholding data matrices to obtain sparse network representations.

PACS numbers: 89.75.Hc, 02.70.Hm, 64.60.aq

Numerous datasets and complex systems are manifest as networks [1]. Consequently, the analysis of networks has far-reaching applications and has improved our understanding of, for example, self-organization in social systems [2] and the brain [3]. Often, a natural representation is that of a multilayer network (see reviews [4, 5]), whereby different network layers encode different classes of interactions, such as categorical social ties [6], types of critical infrastructure [7], or a temporal network at different instances in time [8]. In principle, the multilayer framework offers a more comprehensive representation of a dataset or system, as compared to an aggregation of network layers that produces a simplified model but does so at the cost of information loss. For example, it has been shown that neglecting the layered structure can lead to severe and unintended consequences regarding structure [9] and dynamics [10–12]. In general, the structure and dynamics of multilayer networks can fundamentally differ from that for single-layer networks [13, 14].

However, layer aggregation also implements an information processing that can yield beneficial results if done in a principled way. For example, network layers are often correlated with one another [15], indicating that they may encode redundant information. In some cases the multilayer framework can be an over-modeling of a system, which can negatively impact the computational and memory requirements for storage and analysis. In such situations, it is beneficial to seek a more concise representation in which certain layers—such as those identified to be repetitive—are aggregated [16, 17]. Identifying sets of repetitive layers amounts to a clustering problem, and it is closely related to the topic of clustering networks in an ensemble of networks [17, 18]. Much remains to be studied regarding *when* it is appropriate to aggregate layers and *how* the aggregation should be implemented. Importantly, we expect answers to such questions to greatly depend on the application at hand.

We study here the effect of layer aggregation on community structure in multilayer networks in which each layer is

drawn from a common stochastic block model (SBM)—that is, they make up a “stratum” of network layers [17]. SBMs are a paradigmatic model [19] for complex structure in networks and are particularly useful for studying limitations on detectability—that is, if the community structure is too weak, it cannot be found upon inspection of the network [20, 21]. This so-called “detectability limit” corresponds to a phase transition that is believed to be independent of the method used to find communities [21–24]. Recently, the detectability limit has been explored for networks with degree heterogeneity [25] and hierarchical structure [26], for temporal networks [27], and for the detection of communities using multi-resolution methods [28]. Despite growing interest in multilayer SBMs [29–32], the effect of layer aggregation on detectability limitations has yet to be explored outside the infinite layer limit [33].

To this end, we study the detectability limitations for single-stratum multilayer SBMs and find that the method of aggregation significantly influences detectability. When the aggregate network corresponds to the summation of the adjacency matrices encoding the network layers, aggregation always improves detectability. In particular, the detectability limit vanishes with increasing L and decays as $\mathcal{O}(L^{-1/2})$. Because the summation of L adjacency matrices can often yield a weighted and dense network—which, in practice, increases the computational complexity of community detection [34]—we also study binary adjacency matrices obtained by thresholding the summation of matrices at some value. We find that the detectability limit is very sensitive to the choice of threshold; however, there exist optimal thresholds (e.g., the average edge probability for the case of bi-partitioning equal-sized communities) in which the detectability limit also decays as $\mathcal{O}(L^{-1/2})$. These results are unexpected given the amount of information that is discarded by aggregation and thresholding; they support the use of thresholding data matrices so as to produce sparse networks—a practice that is commonplace but for which the effects are not well understood.

We begin by describing a single-stratum multilayer SBM. We consider N nodes divided into K communities, and we denote by $c_i \in \{1, \dots, K\}$ the community index for each node $i \in \{1, \dots, N\}$. The multilayer network is defined by L layers encoded by a set of adjacency matrices, $\{A^{(l)}\}$, where $A_{ij}^{(l)} = 1$ if (i, j) is an edge in layer l and $A_{ij}^{(l)} = 0$ otherwise. The probability of edge (i, j) in layer l is given by $\Pi_{c_i c_j} \in [0, 1]$, where Π is a $K \times K$ matrix. Note that the nodes are identical in every layer and edges only connect nodes in the same layer, which is a particular type of multilayer network known as a multiplex network [4, 5].

The detectability of community structure relates to the ability to recover the nodes' community labels $\{c_i\}$. To connect to previous literature on detectability [21–24], we focus on the case of $K = 2$ communities of equal size with edge probabilities given by $\Pi_{11} = \Pi_{22} = p_{in}$ and $\Pi_{12} = \Pi_{21} = p_{out}$. We assume $p_{in} \geq p_{out}$ to study “assortative” community structure, in which there is a prevalence of edges between nodes in the same community [35]. In this case, and assuming the network is sparse, the detectability limit is characterized [22, 23] by the solution (Δ^*, ρ) to

$$N\Delta = \sqrt{4N\rho}, \quad (1)$$

where $\Delta = p_{in} - p_{out}$ is the difference in probability and $\rho = (p_{in} + p_{out})/2$ is the mean edge probability. For given ρ , the communities are detectable only when the presence of community structure is sufficiently strong, $\Delta > \Delta^*$.

In this Letter, we study the behavior of Δ^* for two methods of aggregating layers of a single-stratum multilayer SBM. We define the *summation* (SUM) network as the multigraph corresponding to the weighted adjacency matrix $\bar{A} = \sum_l A^{(l)}$. We also define a family of *thresholded* networks which correspond to the unweighted adjacency matrices $\{\hat{A}^{(\tilde{L})}\}$ that are obtained by applying a threshold $\tilde{L} \in \{1, \dots, L\}$ to the entries of \bar{A} . That is, for each \tilde{L} we define $\hat{A}_{ij}^{(\tilde{L})} = 1$ if $\bar{A}_{ij} \geq \tilde{L}$ and $\hat{A}_{ij}^{(\tilde{L})} = 0$ otherwise. Of particular interest are the cases $\tilde{L} = L$ and $\tilde{L} = 1$, which respectively correspond to applying logical AND and OR operations to the set of binary variables $\{A_{ij}^{(l)}\}$ for fixed (i, j) and $l \in \{1, \dots, L\}$. We refer to these limiting cases as the AND and OR networks, respectively.

Following [23, 26], we study the detectability limit for the layer-aggregated networks using random matrix theory [36, 37]. This approach is particularly suited for analyzing detectability limitations since community labels $\{c_i\}$ can be identified using spectral partitioning and phase transitions in detectability correspond to the disappearance of gaps between extremal and bulk eigenvalues. We develop theory based on the modularity matrix [38], defined entry-wise for the summation network by $\bar{B}_{ij} = \bar{A}_{ij} - \rho L$. Note that we do not use the configuration model as the null model. Instead, the appropriate null model is an Erdős-Rényi multigraph in which the expected number of edges between any pair of nodes is ρL .

To identify the detectability limit for the summation network, we study the distribution of real eigenvalues $\{\lambda_i\}$ of

\bar{B} (in descending order). Because \bar{B} is a rank-one perturbation to random matrix \bar{A} , its spectra may be studied through that of \bar{A} [36]. The entries \bar{A}_{ij} are independent random variables following a binomial distribution, $P(\bar{A}_{ij} = a) = f(a; L, \Pi_{c_i c_j}) = \binom{L}{a} \Pi_{c_i c_j}^a (1 - \Pi_{c_i c_j})^{L-a}$ with mean $L\Pi_{c_i c_j}$ and variance $L\Pi_{c_i c_j}(1 - \Pi_{c_i c_j})$. In what follows, we restrict our attention to an SBM with two equal-sized communities and large N . Provided that there is sufficiently large variance in the edge probabilities (i.e., $NL\rho(1 - \rho) \gg 1$), we find that the limiting $N \rightarrow \infty$ distribution of bulk eigenvalues for \bar{B} is given by a semi-circle distribution [23, 26], $P(\lambda_i = z) = \sqrt{4NL\rho(1 - \rho) - z^2} / (2\pi NL\rho(1 - \rho))$. The boundary of the bulk eigenvalues corresponds to the second-largest eigenvalue:

$$\lambda_2 = \sqrt{4NL\rho(1 - \rho)}. \quad (2)$$

In the regime where communities are detectable, the largest eigenvalue is an isolated eigenvalue:

$$\lambda_1 = NL\Delta/2 + 2\rho(1 - \rho)/\Delta. \quad (3)$$

The eigenvector \mathbf{v} corresponding to λ_1 gives the spectral bipartition—the inferred community label of node i is determined by the sign of v_i —and provided that the largest eigenvalue corresponds to this isolated eigenvalue, λ_1 , the eigenvector entries $\{v_i\}$ are correlated with the community labels $\{c_i\}$. The detectability limit is found by equating λ_1 and λ_2 , marking the disappearance of the gap between the isolated eigenvalue λ_1 and the bulk eigenvalues, thus yielding a modified detectability equation:

$$NL\Delta = \sqrt{4NL\rho(1 - \rho)}. \quad (4)$$

Note that Eqs. (2)–(4) do not assume the network to be sparse. Note also for $L = 1$ that Eq. (4) recovers Eq. (1) in the limit $\rho \rightarrow 0$ [i.e., for sparse networks, $\rho(1 - \rho) \approx \rho$]. Defining $p_{in}^* = \rho + \Delta^*/2$ and $p_{out}^* = \rho - \Delta^*/2$, we find for fixed ρ and increasing N and/or L that $p_{in}^* \rightarrow \rho$, $p_{out}^* \rightarrow \rho$, and $\Delta^* \rightarrow 0$, decaying as $\mathcal{O}(1/\sqrt{NL})$. In other words, the detectability limit vanishes for the summation network as the number of layers, L , increases. The cause of this behavior is that the largest eigenvalue λ_1 scales linearly with L , whereas the range of bulk eigenvalues scales more slowly as \sqrt{L} .

For comparison, we now study Δ^* for the thresholded networks, which correspond to single-layer SBMs in which the community labels $\{c_j\}$ are identical to those of the multilayer SBM, but the block edge probabilities are given by new matrices, $\{\hat{\Pi}^{(\tilde{L})}\}$, for $l \in \{1, \dots, L\}$. These encode *effective* edge probabilities after summation and thresholding as given by $\hat{\Pi}_{nm}^{(\tilde{L})} = 1 - F(\tilde{L} - 1; L, \Pi_{nm})$, where $F(a; L, p)$ is the cumulative distribution function for the binomial distribution $f(a; L, p)$. For the AND and OR networks, the effective probabilities are $\hat{\Pi}_{nm}^{(L)} = \Pi_{nm}^L$ and $\hat{\Pi}_{nm}^{(1)} = 1 - (1 - \Pi_{nm})^L$, respectively. For the two-community SBM that we study here,

the effective probabilities are $\hat{p}_{in}^{(\tilde{L})} = 1 - F(\tilde{L} - 1; L, p_{in})$, $\hat{p}_{out}^{(\tilde{L})} = 1 - F(\tilde{L} - 1; L, p_{out})$, $\hat{\Delta}^{(\tilde{L})} = \hat{p}_{in}^{(\tilde{L})} - \hat{p}_{out}^{(\tilde{L})}$, and $\hat{\rho}^{(\tilde{L})} = (\hat{p}_{in}^{(\tilde{L})} + \hat{p}_{out}^{(\tilde{L})})/2$. Given these effective probabilities, we solve for the detectability limit by substituting $\hat{\Delta}^{(\tilde{L})} \mapsto \Delta$ and $\hat{\rho}^{(\tilde{L})} \mapsto \rho$ into Eq. (4) (with $L = 1$) and numerically solving (Δ^*, ρ) using a root-finding algorithm. Note that this solution solves $N\hat{\Delta}^{(\tilde{L})} = \sqrt{4N\hat{\rho}^{(\tilde{L})}(1 - \hat{\rho}^{(\tilde{L})})}$ and it is typically the case that $N\Delta \neq \sqrt{4N\rho(1 - \rho)}$ (i.e., the detectability equation holds for the effective probabilities and not the single-layer probabilities). Note also that the modularity matrix for the thresholded networks is defined using the effective mean edge probability, $\hat{B}_{ij}^{(\tilde{L})} = \hat{A}_{ij}^{(\tilde{L})} - \hat{\rho}^{(\tilde{L})}$.

In Figs. 1(A)–(B), we show Δ^* versus the mean edge probability ρ for the different methods of aggregation. We show results for $N = 1000$ nodes with (A) $L = 4$ and (B) $L = 16$. The red dot-dashed curves are identical in both panels and indicate Δ^* for a single layer. The blue dashed curves indicate Δ^* for the summation network; note that the curve in (B) corresponds to the curve in panel (A) rescaled by a factor of $1/2$. In both panels, we show by solid lines the solutions Δ^* for the thresholded networks with thresholds $\tilde{L} \in \{1, \dots, L\}$. It is evident that the solution curves shift from smaller to larger values of ρ (i.e., left to right) as \tilde{L} increases from 1 to L . This is most evident by comparing Δ^* for the limiting cases of the AND ($\tilde{L} = L$, gold circles) and OR ($\tilde{L} = 1$, cyan squares) networks. We find when ρ is large that the AND (OR) network has a relatively small (large) detectability limit; in contrast, when ρ is small the AND (OR) network has a relatively large (small) detectability limit. In other words, combining edges using the AND operation is beneficial for dense networks, whereas the OR operation is beneficial for sparse networks.

For a given ρ , it is interesting to ask which threshold leads to the smallest detectability limit Δ^* . A related and perhaps more pertinent question is whether there are choices of ρ and \tilde{L} for which the detectability limit vanishes as $\mathcal{O}(L^{-1/2})$ with increasing L —that is, a behavior similar to that of the summation network. To this end, we study the threshold $\tilde{L} = \lceil \rho L \rceil$, which we find to be the optimal threshold for most values of ρ . This choice is also convenient as it only requires knowledge of the mean edge probability, ρ , which is easy to obtain in practice. In Fig. 1(C), we plot by orange dots the solution Δ^* versus ρ for $L = 4$ and $\tilde{L} = \lceil \rho L \rceil$, which lies along the solution curves for $\tilde{L} \in \{1, \dots, L\}$ (solid curves). Note that, in contrast to Figs. 1(A)–(B), the vertical axis is normalized by the \sqrt{NL} scaling of Δ^* for the summation network.

In Fig. 1(D), we plot Δ^* versus ρ for threshold $\tilde{L} = \lceil \rho L \rceil$ with $L = 4$ (orange dots) and $L = 64$ (green triangles). These curves align due to the rescaling of the vertical axis by \sqrt{NL} . In fact, we find that these solutions Δ^* collapse onto a single curve in the large L limit. Specifically, as L increases, the binomial distribution $f(a; L, p)$ limits to $g(a; Lp, Lp(1 - p))$, where $g(a; \mu, \sigma^2)$ is the normal distribution function with mean μ and variance σ^2 . It follows that

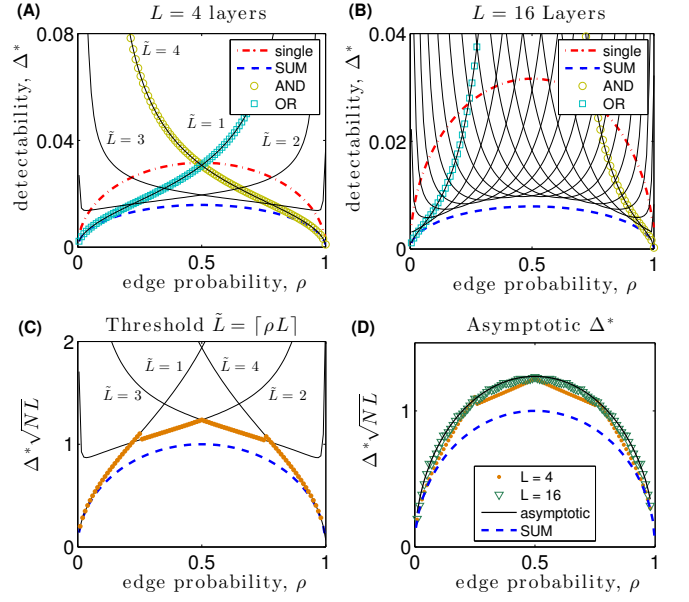


FIG. 1. (Color online) *Enhanced detectability limit Δ^* through layer aggregation.* (A)–(B) We plot Δ^* versus mean edge probability ρ for a single layer (red dot-dashed curves), summation network (blue dashed curves), and thresholded networks with threshold $\tilde{L} \in \{1, \dots, L\}$ (solid curves). We also plot Δ^* for the AND (gold circles) and OR (cyan squares) networks. Results are shown for $N = 1000$ nodes with (A) $L = 4$ and (B) $L = 16$ layers. (C) We show Δ^* versus ρ for thresholded networks with $\tilde{L} = \lceil \rho L \rceil$ (orange dots) and $L = 4$, which lies on the solution curves for thresholded networks with $\tilde{L} \in \{1, \dots, L\}$ (solid curves). (D) We show Δ^* for $\tilde{L} = \lceil \rho L \rceil$ with $L = 4$ (orange dots) and $L = 64$ (green triangles). These piecewise-continuous solutions collapse onto the asymptotic solution (black curve) as L increases. In panels (C)–(D), we additionally plot Δ^* for the summation network (blue dashed curves).

$1 - F(\tilde{L} - 1; L, p)$ limits to $1 - G(\tilde{L} - 1; Lp, Lp(1 - p))$, where $G(a; \mu, \sigma^2)$ is the associated cumulative distribution function. We define $\hat{p}_{in}^{(asym)} = 1 - G(\tilde{L} - 1; Lp_{in}, Lp_{in}(1 - p_{in}))$, $\hat{p}_{out}^{(asym)} = 1 - G(\tilde{L} - 1; Lp_{out}, Lp_{out}(1 - p_{out}))$, $\hat{\Delta}^{(asym)} = \hat{p}_{in}^{(asym)} - \hat{p}_{out}^{(asym)}$, and $\hat{\rho}^{(asym)} = (\hat{p}_{in}^{(asym)} + \hat{p}_{out}^{(asym)})/2$. As before, we substitute $\hat{\Delta}^{(asym)} \mapsto \Delta$ and $\hat{\rho}^{(asym)} \mapsto \rho$ into Eq. (4) (with $L = 1$) and numerically find a solution (Δ^*, ρ) , which we plot in Fig. 1(D) by the black curve. We observe for either increasing N or L that this solution curve Δ^* decays as $\mathcal{O}(1/\sqrt{NL})$. Therefore, the detectability limit vanishes for thresholded networks with threshold $\tilde{L} = \lceil \rho L \rceil$ as L increases.

Next, we further explore the mechanism giving rise to enhanced detectability by studying the effective edge probabilities, $\hat{p}_{in}^{(\lceil \rho L \rceil)} = 1 - F(\lceil \rho L \rceil - 1; L, p_{in})$ and $\hat{p}_{out}^{(\lceil \rho L \rceil)} = 1 - F(\lceil \rho L \rceil - 1; L, p_{out})$. In particular, application of the Chernoff bound [39] yields the inequalities $p_{in}^{(\lceil \rho L \rceil)} \geq 1 - e^{-2L(p_{in} - \rho)^2}$ and $p_{out}^{(\lceil \rho L \rceil)} \leq e^{-2L(p_{out} - \rho)^2}$. It follows that, for fixed p_{in} and p_{out} , the effective edge probabilities have the limiting behavior $\hat{p}_{in}^{(\lceil \rho L \rceil)} \rightarrow 1$ and $\hat{p}_{out}^{(\lceil \rho L \rceil)} \rightarrow 0$ as $L \rightarrow \infty$. In other words, the limiting thresholded network is described by an adjacency matrix with values $A_{ij} = \delta_{c_i c_j}$, where δ_{nm}

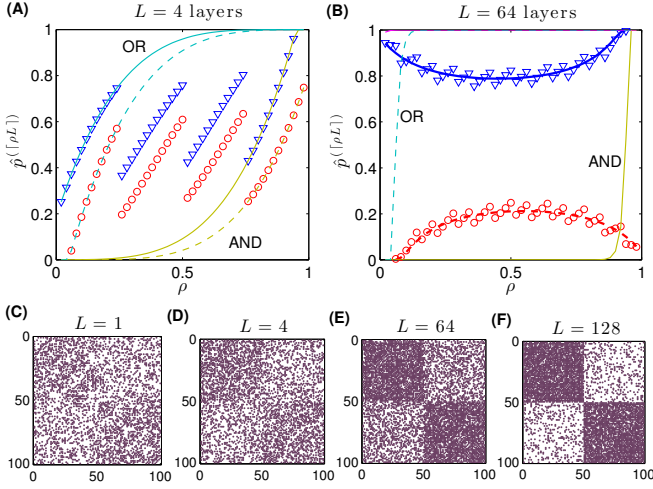


FIG. 2. (Color online) *Effective edge probabilities for thresholded networks.* (A)–(B) Blue triangles and red circles indicate $\hat{p}_{in}^{(\lceil \rho L \rceil)}$ and $\hat{p}_{out}^{(\lceil \rho L \rceil)}$ for $\Delta = 0.1$ (i.e., $p_{in} = \rho + 0.05$ and $p_{out} = \rho - 0.05$) for (A) $L = 4$ and (B) $L = 64$ layers. We also show by gold and cyan curves the effective probabilities for the AND and OR networks, respectively (solid and dashed curves give \hat{p}_{in} and \hat{p}_{out} , respectively). The blue solid and red dashed curves in (B) indicate $\hat{p}_{in}^{(asym)}$ and $\hat{p}_{out}^{(asym)}$. (C)–(F) Adjacency matrices of thresholded networks with $\rho = 0.3$, $\Delta = 0.1$, threshold $\tilde{L} = \lceil \rho L \rceil$ and various L .

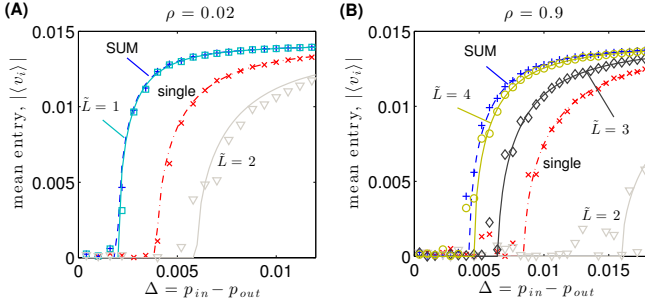


FIG. 3. (Color online) *Phase transition in the dominant eigenvector for the modularity matrix at the detectability limit Δ^* .* The mean eigenvector entry $|\langle v_i \rangle|$ within a community for $N = 5000$ and $L = 4$ with (A) $\rho = 0.02$ and (B) $\rho = 0.9$. Symbols and curves indicate observed values and predicted values given by Eq. (5), respectively.

is the Kronecker delta function.

We illustrate this behavior in Fig. 2. In panels (A)–(B), we plot $\hat{p}_{in}^{(\lceil \rho L \rceil)}$ (blue triangles) and $\hat{p}_{out}^{(\lceil \rho L \rceil)}$ (red circles) versus ρ for $\Delta = 0.1$ with (A) $L = 4$ and (B) $L = 64$. We also plot the effective probabilities \hat{p}_{in} (solid curves) and \hat{p}_{out} (dashed curves) for the AND (gold curves) and OR (cyan curves) networks. In panel (B), we additionally plot the limiting effective probabilities $\hat{p}_{in}^{(asym)}$ (blue solid curve) and $\hat{p}_{out}^{(asym)}$ (red dashed curve). In Figs. 2(C)–(F), we illustrate adjacency matrices of sample thresholded networks for $\rho = 0.3$, $\Delta = 0.1$ and threshold $\tilde{L} = \lceil \rho L \rceil$ for various L . We note that the community structure is undetectable for $L = 1$ since $\Delta^* = 0.1095$; in contrast, it is detectable (and visually apparent) for $L = 128$.

We conclude by studying the dominant eigenvector v of the appropriate modularity matrix, which undergoes a second-order phase transition at Δ^* : $\{v_i\}$ and the community labels $\{c_i\}$ are uncorrelated for $\Delta < \Delta^*$, whereas they are correlated for $\Delta > \Delta^*$. We extend the analysis of [23] to multilayer (and potentially dense) networks and find

$$|\langle v_i \rangle| = \sqrt{1 - \frac{4NL\rho(1-\rho)}{(NL\Delta)^2}}, \quad (5)$$

where $\langle v_i \rangle$ denotes the mean value across nodes within a community. In Fig. 3, we depict the phase transition for v by plotting $|\langle v_i \rangle|$ for various Δ with (A) $\rho = 0.02$ and (B) $\rho = 0.9$. Symbols and curves indicate observed values and predicted values given by Eq. (5), respectively. We show results for a single layer (red \times -symbols), the summation network (blue $+$ -symbols), and thresholded networks (open symbols) with $\tilde{L} \in \{1, 2\}$ in panel (A) and $\tilde{L} \in \{2, 3, 4\}$ in panel (B). We omit results for the other thresholds, for which v doesn't undergo a phase transition within the shown range of Δ .

In this Letter, we studied the limitations on community detection for single-stratum multilayer SBMs. As an illustrative model, we analyzed the effect of layer aggregation on the detectability limit Δ^* for two equal-sized communities and found that aggregation often enhances detectability. When layers are aggregated by summation, detectability is always enhanced and Δ^* vanishes as $\mathcal{O}(L^{-1/2})$. When layers are aggregated by thresholding the summation of matrices, Δ^* depends sensitively on the choice of threshold, \tilde{L} . For $\tilde{L} = \lceil \rho L \rceil$, we found Δ^* to also vanish with increasing L as $\mathcal{O}(L^{-1/2})$. Our analysis relied on random matrix theory for the modularity matrix and can be extended to other matrices [26]. For example, we find Δ^* for the modularity matrix to be identical to that of the adjacency and normalized Laplacian matrices for the networks that we study.

We note that our analysis also describes layer aggregation by taking the mean, $L^{-1} \sum_l A^{(l)}$, since the multiplication of a matrix by a constant (e.g., L^{-1}) simply scales all eigenvalues by that constant. Thus, our results are in excellent agreement with previous work [33] that proved spectral clustering via the mean adjacency matrix to be a consistent estimator for the community labels. Importantly, averaging yields an aggregate network with edge weights that approximate the edge probabilities $\{\Pi_{nm}\}$, and this information can be incorporated into community detection algorithms [33, 40].

Finally, it is commonplace to threshold data matrices so as to construct sparse unweighted networks that can be studied at a lower computational cost. Our research provides insight into this common—yet not well understood—practice. We find the detectability of communities to greatly depend on threshold choice, and in particular, we found the existence of an optimal threshold for the networks that we studied. Due to its widespread usage, it is important that we develop a better understanding of the effects of thresholding. Such research should include, for example, exploring its effect on the de-

tectability of hierarchical community structure [41] and manifold structure [42].

The authors were supported by the NIH (R01HD075712, T32GM067553, T32CA201159) and the James S. McDonnell Foundation (#220020315). The content does not necessarily represent the views of the funding agencies.

* dane.r.taylor@gmail.com

- [1] M. E. J. Newman, *SIAM Rev.* **45**(2), 167–256 (2003).
- [2] J. Moody, *Amer. Soc. Rev.* **69**(2), 213–238 (2004).
- [3] D. S. Bassett *et al.*, *Proc. Natl. Acad. of Sci.* **108**, 7641–8646 (2011).
- [4] S. Boccaletti *et al.*, *Phys. Reports*, **544**(1), 1–122 (2014).
- [5] M. Kivela *et al.*, *J. of Complex Networks* **2**(3), 203–271 (2014).
- [6] D. Krackhardt, *Social Networks* **9**(2), 109–134 (1987).
- [7] Y. Y. Haimes and P. Jiang, *J. of Infrast. Sys.* **7**(1) 1–12 (2001).
- [8] P. Holme and J. Saramäki, *Phys. Reports* **519**(3), 97–125 (2012).
- [9] P. J. Mucha and *et al.*, *Science* **328**(5980), 876–878 (2010).
- [10] R. J. Sánchez-García, E. Cozzo and Y. Moreno, *Phys. Rev. E* **89**(5), 052815 (2014).
- [11] A. Sole-Ribalta *et al.*, *Phys. Rev. E* **88**(3), 032807 (2013).
- [12] C. D. Brummitt, R. M. D’Souza and E. A. Leicht, *Proc. Natl. Acad. Sci.* **109**(12), E680–E689 (2012).
- [13] A. Bashan, Y. Berezin, S. V. Buldyrev and S. Havlin, *Nat. Phys.* **9**(10), 667–672 (2013).
- [14] F. Radicchi and A. Arenas, *Nat. Phys.* **9**(11), 717–720 (2013).
- [15] G. Menichetti, D. Remondini and G. Bianconi, *Phys. Rev. E* **90**(6) 062817 (2014).
- [16] M. De Domenico, V. Nicosia, A. Arenas and V. Latora, *et al.*, *Nat. Comms.* **6**, 6864 (2015).
- [17] N. Stanley, S. Shai, D. Taylor, P. J. Mucha, Preprint available online at <http://arxiv.org/abs/1507.01826> (2015).
- [18] J.-P. Onnela *et al.* *Phys. Rev. E* **86**, 036104 (2012).
- [19] A. Lancichinetti, S. Fortunato and F. Radicchi, *Phys. Rev. E* **78**(4), 046110 (2008).
- [20] A. Lancichinetti and S. Fortunato, *Phys. Rev. E* **84**(6), 066122 (2011).
- [21] J. Reichardt and M. Leone, *Phys. Rev. Lett.* **101**, 078701 (2008).
- [22] A. Decelle, F. Krzakala, C. Moore and L. Zdeborová, *Phys. Rev. Lett.* **107**(6), 065701 (2011).
- [23] R. R. Nadakuditi and M. E. J. Newman, *Phys. Rev. E* **87**(1), 012803 (2013).
- [24] E. Abbe, A. S. Bandeira and G. Hall, Preprint available online at <http://arxiv.org/abs/1405.3267> (2014).
- [25] F. Radicchi, *Phys. Rev. E* **88**(1), 010801 (2013).
- [26] T. P. Peixoto, *Phys. Rev. Lett.* **111**(9), 098701 (2013).
- [27] A. Ghasemian *et al.*, Preprint available online at <http://arXiv.org/abs/1506.06179> (2015).
- [28] T. Kawamoto and Y. Kabashima, Preprint available online at <http://arxiv.org/abs/1509.06484> (2015).
- [29] T. Valles-Catala, F. A. Massucci, R. Guimera, and M. Sales-Pardo, Preprint available online at <http://arxiv.org/abs/1411.1098> (2014).
- [30] S. Paul and Y. Chen, Preprint available online at <http://arxiv.org/abs/1506.02699> (2015).
- [31] P. Barbillon, S. Donnet, E. Lazega, and A. Bar-Hen, Preprint available online at <http://arxiv.org/abs/1501.06444> (2015).
- [32] T. P. Peixoto, Preprint available online at <http://arxiv.org/abs/1504.02381> (2015).
- [33] Q. Han, K. Xu, and E. Airoldi, *Proc. of the 32nd Int. Conf. on Machine Learn.*, 1511–1520 (2015).
- [34] C. Aicher, A. Z. Jacobs and A. Clauset, *J. of Complex Networks* **3**(2), 221–248 (2015).
- [35] M. P. Rombach *et al.*, *SIAM J. on A. Math.* **74**(1) 167–190 (2014).
- [36] F. Benaych-Georges and R. R. Nadakuditi, *Adv. in Math.* **227**, 494 (2011).
- [37] R. R. Nadakuditi and M. E. J. Newman, *Phys. Rev. Lett.* **108**(18), 188701 (2012).
- [38] M. E. J. Newman and M. Girvan, *Phys. Rev. E* **69**(2), 026113 (2004).
- [39] T. Hagerup, *Info. Proc. Lett.* **33**(6), 305 (1990).
- [40] T. Martin, B. Ball and M. E. J. Newman, Preprint available online at <http://arxiv.org/abs/1506.05490> (2015).
- [41] T. P. Peixoto, *Phys. Rev. X* **4**, 011047 (2014).
- [42] D. Taylor *et al.*, *Nat. Comm.* **6**, 7723 (2015).